

# Numerical investigation of short-pulse laser radiation propagation in a turbulent atmosphere

V.A. Banakh, L.O. Gerasimova, I.N. Smalikho

**Abstract.** An algorithm is presented for the numerical simulation of short-pulse optical radiation propagation in a turbulent atmosphere on the basis of the solution to the parabolic wave equation for the complex spectral amplitude of the wave field by the split-step method. We present examples of the use of this algorithm for simulating the propagation of a pulsed coherent spatially limited beam and a plane wave. It is shown that in the regime of strong optical turbulence the relative variance of fluctuations of energy density of femtosecond radiation becomes much smaller than the relative variance of the intensity of cw radiation.

**Keywords:** short-pulse radiation, complex spectral amplitude, turbulent atmosphere, parabolic wave equation, split-step method.

## 1. Introduction

The development of femtosecond optics and the possibility of its application in atmospheric problems [1] determine the importance of studying short-pulse laser radiation propagation in a turbulent atmosphere [2–4]. In the case of narrow-band cw or pulsed radiation, the problem of the optical wave propagation in a turbulent atmosphere is solved by using the equations for the statistical moments of the complex wave-field amplitude, obtained in the Markov approximation from the stationary parabolic wave equation [5–8]. A rigorous solution of these equations under arbitrary turbulent propagation conditions is possible only for the second-order coherence function, whereas for higher-order statistical moments only asymptotic solutions in the regime of weak and strong intensity fluctuations are known [7, 8]. Moreover, even the equation for the second statistical moment has no exact solution if it is written for the fields at different frequencies, which is required for solving the problems of pulsed radiation propagation in a turbulent atmosphere. The solution of statistical problems of optical radiation propagation under arbitrary turbulent conditions is possible on the basis of numerical methods, in particular the split-step method [9].

In the case of broadband radiation, when the pulse duration can be equal to several wave periods, investigation of laser pulse propagation in a turbulent atmosphere should be based on the nonstationary wave equation [10]. From the lat-

ter in the paraxial approximation one can derive an equation for the coherence function (statistical moments) of the spectral field amplitudes of the laser beam. However, the solution of these equations at arbitrary values of the problem parameters is possible only for the second-order coherence function. Peculiarities of the diffraction spreading of broadband pulsed laser beams in the absence of turbulence are considered in [11–17].

In this paper, the propagation of short-pulse laser radiation in a turbulent atmosphere is studied by using a numerical simulation algorithm constructed on the basis of the solution of the parabolic wave equation for the complex spectral amplitude of the wave field by the split-step method. We describe the algorithm and present the examples of modelling. By using the proposed algorithm and Monte Carlo method we analyse the relative variance of fluctuations of energy density of radiation for the regimes of a plane wave and a narrow laser beam.

## 2. Parabolic wave equation

Let pulsed laser radiation propagate in a turbulent atmosphere along the axis  $x \geq 0$ . By  $E(x, \rho, t)$  we denote the complex electric field strength of the wave at point  $(x, \rho)$  at time  $t$  ( $\rho = \{y, z\}$  is the radius-vector in a plane perpendicular to the optical axis). We assume that laser radiation is fully coherent, and the strength  $E(x, \rho, t)$  in the initial plane has the form

$$E(0, \rho, t) = E_0 \exp\left(-\frac{\rho^2}{2a_0^2} - \frac{t^2}{2\tau_0^2} - 2\pi j f_0 t + j\psi_0\right), \quad (1)$$

where  $E_0 = E(0, 0, 0)$  is the amplitude at the axis;  $a_0$  and  $\tau_0$  are the initial beam radius and pulse duration determined by a decrease in  $|E(0, \rho, 0)|^2$  and  $|E(0, 0, t)|^2$ , respectively, to the  $e^{-1}$  level;  $j = \sqrt{-1}$ ;  $f_0$  is the frequency at the maximum of the emission spectrum; and  $\psi_0$  is the wave phase, which is independent of  $\rho$  and  $t$ . In this case, the pulse duration  $\tau_p(x)$ , determined by a decrease in

$$\int_{-\infty}^{+\infty} d^2\rho |E(x, \rho, t)|^2$$

to the 1/2 level from the right and left of the maximum  $t = t_{\max}$  in the plane  $x = 0$  is related to  $\tau_0$  by the equation  $\tau_p(0) = 2\sqrt{\ln 2} \tau_0$ .

In the absence of the nonlinear interaction of radiation with the medium and if we can neglect the absorption of radiation by air and aerosol particles, the complex spectral amplitude of the wave field

V.A. Banakh, L.O. Gerasimova, I.N. Smalikho V.E. Zuev Institute of Atmospheric Optics, Siberian Branch, Russian Academy of Sciences, pl. Akad. Zueva 1, 634021 Tomsk, Russia; e-mail: banakh@iao.ru

Received 10 July 2014; revision received 10 September 2014  
Kvantovaya Elektronika 45 (3) 258–264 (2015)  
Translated by I.A. Ulitkin

$$\tilde{E}(x, \boldsymbol{\rho}, f) = \int_{-\infty}^{+\infty} dt E(x, \boldsymbol{\rho}, t) \exp(2\pi j f t) \quad (2)$$

is described by the equation [10]

$$\begin{aligned} \frac{\partial^2 \tilde{E}(x, \boldsymbol{\rho}, f)}{\partial x^2} + \Delta_{\perp} \tilde{E}(x, \boldsymbol{\rho}, f) \\ + \left( \frac{2\pi f}{c} \right)^2 n^2(x, \boldsymbol{\rho}, f) \tilde{E}(x, \boldsymbol{\rho}, f) = 0 \end{aligned} \quad (3)$$

with the boundary condition

$$\tilde{E}(0, \boldsymbol{\rho}, f) = \sqrt{2\pi} \tau_0 E_0 \exp \left[ -\frac{\boldsymbol{\rho}^2}{2a_0^2} - \frac{(f-f_0)^2}{2\sigma_f^2} + j\psi_0 \right], \quad (4)$$

where  $\Delta_{\perp} = \partial^2/\partial y^2 + \partial^2/\partial z^2$  is the transverse Laplace operator;  $c$  is the speed of light in vacuum;  $n(x, \boldsymbol{\rho}, f)$  is the refractive index of air, which depends on the radiation wavelength  $\lambda = cf$ ; and  $\sigma_f = (2\pi\tau_0)^{-1}$  is the width of the emission spectrum, which is determined by a decrease in  $|\tilde{E}(0, 0, f)|^2$  from the maximum to the  $e^{-1}$  level.

We assume that the refractive index of air along the propagation path is a statistically homogeneous field. Thus, we make use of the model of dry air for it [6]

$$n(x, \boldsymbol{\rho}, f) = 1 + 10^{-6} \frac{P_a}{T(x, \boldsymbol{\rho})} \left[ 77.6 + \frac{0.584}{\lambda_0^2} \left( \frac{f}{f_0} \right)^2 \right], \quad (5)$$

where  $P_a$  is the atmospheric pressure in millibars;  $T(x, \boldsymbol{\rho})$  is the temperature of air in Kelvin; and  $\lambda_0 = cf_0$  (in  $\mu\text{m}$ ). Given the fact that the temperature  $\langle T \rangle$  averaged over an ensemble of realisations in the atmosphere is much larger than the turbulent fluctuations of temperature  $T'(x, \boldsymbol{\rho}) = T(x, \boldsymbol{\rho}) - \langle T \rangle$  [6], the refractive index can be represented as

$$n(x, \boldsymbol{\rho}, f) = \langle n(f) \rangle + n'(x, \boldsymbol{\rho}, f), \quad (6)$$

where

$$\langle n(f) \rangle = 1 + 10^{-6} \frac{P_a}{\langle T \rangle} \left[ 77.6 + \frac{0.584}{\lambda_0^2} \left( \frac{f}{f_0} \right)^2 \right] \quad (7)$$

is the average value and

$$n'(x, \boldsymbol{\rho}, f) = [1 - \langle n(f) \rangle] T'(x, \boldsymbol{\rho}) / \langle T \rangle \quad (8)$$

are the fluctuations in the refractive index caused by turbulent variations of the air temperature. Taking into account the fact that  $|n'(x, \boldsymbol{\rho}, f)| \ll 1$  in the atmosphere [5], we will use from (3) the approximate equality

$$n^2(x, \boldsymbol{\rho}, f) = \langle n(f) \rangle^2 [1 + 2n'(x, \boldsymbol{\rho}, f) / \langle n(f) \rangle]. \quad (9)$$

If the effect of turbulent fluctuations of the refractive index and radiation diffraction on the spectral amplitude of the strength  $\tilde{E}(x, \boldsymbol{\rho}, f)$  is negligible (plane wave regime), we can neglect in (3) the second term and replace  $n(x, \boldsymbol{\rho}, f)$  by  $\langle n(f) \rangle$ . Then, the solution of equation (3) has the form [10]

$$\tilde{E}(x, \boldsymbol{\rho}, f) = \tilde{E}(0, \boldsymbol{\rho}, f) \exp[2\pi j f \langle n(f) \rangle x / c]. \quad (10)$$

The radiation power is defined as

$$P(x, t) = \int_{-\infty}^{+\infty} d^2 \boldsymbol{\rho} I(x, \boldsymbol{\rho}, t),$$

where  $I(x, \boldsymbol{\rho}, t) = |E(x, \boldsymbol{\rho}, t)|^2$  is the intensity (power density) of radiation and, in accordance with (2),

$$E(x, \boldsymbol{\rho}, t) = \int_{-\infty}^{+\infty} df \tilde{E}(x, \boldsymbol{\rho}, f) \exp(-2\pi j f t). \quad (11)$$

From (4), (10) and (11) we obtain

$$\begin{aligned} P(x, t) = 2(\pi\tau_0 a_0 E_0)^2 \\ \times \left| \int_{-\infty}^{+\infty} df \exp \left\{ -\frac{(f-f_0)^2}{2\sigma_f^2} - 2\pi j [t - \langle n(f) \rangle x / c] f \right\} \right|^2, \end{aligned} \quad (12)$$

where  $\langle n(f) \rangle$  is described by formula (7). The integral in (12) can be calculated analytically if we use the expansion of the function  $\Omega(f) = f \langle n(f) \rangle$  in the Taylor series in the vicinity of point  $f = f_0$  and restrict our consideration only to the first three terms of the series. [10] As a result, the dependence of the pulse duration on the distance  $x$  has the form

$$\tau_p(x) = 2\sqrt{\ln 2} \tau_0 \sqrt{1 + \left( \frac{3}{\pi} \mu \frac{x}{c\tau_0^2 f_0} \right)^2}, \quad (13)$$

where the dimensionless parameter  $\mu$  is given by the expression

$$\mu = 10^{-6} \frac{P_a}{\langle T \rangle} \frac{0.584}{\lambda_0^2}. \quad (14)$$

In Eqn (14)  $P_a$ ,  $T$  and  $\lambda_0$  are given in the same units as in formula (5).

According to calculations by formulas (13) and (14) at  $\tau_0 = 3$  fs [ $\tau_p(0) = 5$  fs],  $\lambda_0 = 1$   $\mu\text{m}$  ( $f_0 = 300$  THz),  $P_a = 1013$  mbar and  $\langle T \rangle = 288$  K, the pulse duration at a distance  $x = 1$  km is 2358 times greater than the initial duration of the pulse [ $c\tau_p(x) = 1.5$   $\mu\text{m}$  at  $x = 0$  and  $c\tau_p(x) = 3.5$  mm at  $x = 1$  km].

Below we will take into account the diffraction of the laser beam and its distortions in turbulent inhomogeneities of the refractive index. By analogy with (10) we represent the spectral amplitude of the wave field strength in the form

$$\tilde{E}(x, \boldsymbol{\rho}, f) = U(x, \boldsymbol{\rho}, f) \exp[2\pi j f \langle n(f) \rangle x / c]. \quad (15)$$

After substituting (15) into (3) we obtain the equation for the complex spectral amplitude  $U(x, \boldsymbol{\rho}, f)$ , where we can neglect the term  $\partial^2 U(x, \boldsymbol{\rho}, f) / \partial x^2$ . As a result, in replacing  $\langle n(f) \rangle$  by unity (because the refractive index of air is different from unity in the fourth decimal place) and  $n'(x, \boldsymbol{\rho}, f)$  by  $n(x, \boldsymbol{\rho})$  (in a dispersive medium the dependence of turbulent fluctuations of the refractive index on the frequency  $f$  can be ignored), with allowance for (9) we arrive at the parabolic wave equation

$$\begin{aligned} j \frac{4\pi f}{c} \frac{\partial U(x, \boldsymbol{\rho}, f)}{\partial x} + \Delta_{\perp} U(x, \boldsymbol{\rho}, f) + 2 \left( \frac{2\pi f}{c} \right)^2 \\ \times n'(x, \boldsymbol{\rho}) U(x, \boldsymbol{\rho}, f) = 0. \end{aligned} \quad (16)$$

Because  $U(0, \boldsymbol{\rho}, f) = \tilde{E}(0, \boldsymbol{\rho}, f)$ , the boundary condition for equation (16) is defined by formula (4).

### 3. Split-step method for the numerical solution of the parabolic wave equation

To solve numerically equation (16) we will use the split-step method [9], whose essence, as applied to our case, is as follows. The entire propagation path of length  $L$  is divided into  $N$  layers with a thickness  $\Delta x = L/N$ . The complex spectral amplitude  $U(x, \rho, f)$  for each frequency  $f$ , where  $x_i = i\Delta x$  ( $i = 0, 1, \dots, N$ ), is sequentially calculated by passing from layer to layer. Equation (16) at the end of the  $i$ th layer ( $x \in [x_{i-1}, x_{i-1} + \Delta x]$ ) is solved in two stages.

1. Only the phase distortions produced by a wave at a frequency  $f$  when it passes through turbulent inhomogeneities of the refractive index inside the layer are taken into account. Then, the spectral amplitude of the wave, which is denoted by  $U_1(x_i, \rho, f)$ , is described by equation (16), in which the second term is equal to zero and  $U(x_i, \rho, f)$  is replaced by  $U_1(x_i, \rho, f)$ , with the boundary condition

$$U_1(x_{i-1}, \rho, f) = U(x_{i-1}, \rho, f). \quad (17)$$

Taking into account (17), the solution of this equation has the form

$$U_1(x_i, \rho, f) = U(x_{i-1}, \rho, f) \exp[j\Psi_i(\rho, f)], \quad (18)$$

where

$$\Psi_i(\rho, f) = (2\pi f/c) \int_0^{\Delta x} dx' \tilde{n}(x_{i-1} + x', \rho) \quad (19)$$

is a random phase screen.

2. Only the wave diffraction is taken into account. Then, the spectral amplitude of the wave field, which is denoted by  $U_2(x_i, \rho, f)$ , is described by equation (16), in which the third term is equal to zero and  $U(x_i, \rho, f)$  is replaced by  $U_2(x_i, \rho, f)$ , with the boundary condition

$$U_2(x_{i-1}, \rho, f) = U_1(x_i, \rho, f). \quad (20)$$

Applying the direct two-dimensional Fourier transform

$$\tilde{U}_2(x, \kappa, f) = \int_{-\infty}^{+\infty} d^2\rho U_2(x, \rho, f) \exp(-2\pi j\kappa\rho), \quad (21)$$

where  $\kappa = \{\kappa_x, \kappa_z\}$  is the vector of spatial frequencies, from the equation for  $U_2$  we obtain an ordinary differential equation for  $\tilde{U}_2$ , whose solution with allowance for (20) and (21) has the form

$$\tilde{U}_2(x_i, \kappa, f) = \tilde{U}_2(x_{i-1}, \kappa, f) \exp(-j\pi\kappa^2 \Delta x c/f), \quad (22)$$

where

$$\tilde{U}_2(x_{i-1}, \kappa, f) = \int_{-\infty}^{+\infty} d^2\rho U_1(x_i, \rho, f) \exp(-2\pi j\kappa\rho). \quad (23)$$

Finally, the spectral amplitude  $U(x_i, \rho, f) = U_2(x_i, \rho, f)$  is calculated by applying an inverse two-dimensional Fourier transform:

$$U(x_i, \rho, f) = \int_{-\infty}^{+\infty} d^2\kappa \tilde{U}_2(x_i, \kappa, f) \exp(2\pi j\kappa\rho). \quad (24)$$

From the simulated spectral amplitudes  $U(L, \rho, f)$  we can calculate the spectral intensity

$$S_I(L, \rho, f) = |U(L, \rho, f)|^2, \quad (25)$$

the spectral power

$$S_P(L, f) = \int_{-\infty}^{+\infty} d^2\rho S_I(L, \rho, f) \quad (26)$$

and radiation energy density

$$W(L, \rho) = \int_{-\infty}^{+\infty} dt I(L, \rho, t) = \int_{-\infty}^{+\infty} dt |E(L, \rho, t)|^2. \quad (27)$$

From (11), (15), (25) and (27) we obtain the relation

$$W(L, \rho) = \int_{-\infty}^{+\infty} df S_I(L, \rho, f). \quad (28)$$

It can be shown that if the radiation energy absorption on the propagation path of length  $L$  is insignificant,  $S_P(L, f)$ , unlike  $S_I(L, \rho, f)$ , does not depend on  $L$ , i.e.,  $S_P(L, f) = S_P(0, f)$  [10]. To take absorption into account, we should multiply the calculated values of  $U(x_i, \rho, f)$  by  $\exp[-\alpha(f)\Delta x/2]$  in each layer of the propagation path, where  $\alpha(f)$  is the absorption coefficient of the radiation energy by atmospheric air and aerosol.

### 4. Numerical simulation of random phase screens

For numerical simulation of random realisations of a phase screen,  $\Psi_i(\rho, f)$ , we need to know its statistical properties. We assume that inside the  $i$ th layer of the propagation path the probability density  $p(\Psi_i)$  has the normal distribution. The main contribution to the distortion of the laser beam propagating in a turbulent atmosphere is made by the inhomogeneities of the refractive index, the structure of which obeys the fundamental Kolmogorov–Obukhov law [5]. Therefore, for the structure function of the wave phase

$$\begin{aligned} D_\Psi(r, f) &= \langle [\Psi_i(\rho + r, f) - \Psi_i(\rho, f)]^2 \rangle \\ &= 2 \int_{-\infty}^{+\infty} d^2\kappa S_\Psi(\kappa, f) [1 - \exp(2\pi j\kappa\rho)] \end{aligned} \quad (29)$$

we use the model spectrum of phase fluctuations  $S_\Psi(\kappa, f)$  in the form [5–8, 18]

$$S_\Psi(\kappa, f) = 0.382 C_n^2 \Delta x (f/c)^2 |\kappa|^{-11/3}, \quad (30)$$

where  $C_n^2$  is structure characteristic of turbulent fluctuations of the refractive index of air.

Using (30) the independent random realisations  $\Psi_i(\rho, f_0)$  ( $\langle \Psi_i \Psi_{i \neq i} \rangle = 0$ ) are simulated on the  $M \times M$  computational grid with a step  $h$  by applying a two-dimensional fast Fourier transform (FFT) to an array of complex spectral phase amplitudes generated on a computer [9, 18–20]. For the realisation of the random phase screen at other frequencies  $f$  use is made of the relation  $\Psi_i(\rho, f) = (f/f_0) \Psi_i(\rho, f_0)$ .

After substituting (30) into (29) and calculating the integral we obtain the well-known expression [6]

$$D_\Psi(r, f) = 2.92 C_n^2 \Delta x (2\pi f/c)^2 |r|^{5/3}. \quad (31)$$

Due to the fact that  $h > 0$  and  $Mh < \infty$ , the structure function of the simulated phase screens differs from those obtained by calculation using formula (31). Here  $h$  and  $Mh/2$  can be considered analogous of the inner and outer scales of turbulence, respectively. For the structure function of the simulated phase screen to coincide with the results of calculations by formula (31) at  $h \ll |r| \leq Mh$ , we can use the method of sub-harmonics [19, 20].

## 5. Numerical simulation of random realisations and calculation of statistical characteristics of radiation energy density

Calculations of the spectral amplitude  $U(x_i, \rho, f)$  by the split-step method and algorithm of generation of random phase screens are made in each layer of the path for  $K + 1$  beams at frequencies  $f = f_0 + (k - K/2)\Delta f$  ( $k = 0, 1, \dots, K$ ,  $\Delta f$  is the frequency step) in uniform grid nodes  $\rho = \{(m_y - M/2)h, (m_z - M/2)h\}$  ( $m_{y,z} = 0, 1, \dots, M - 1$ ). To calculate  $\kappa = \{k_y/(Mh), k_z/(Mh)\}$  ( $k_{y,z} = 0, 1, \dots, M - 1$ ) and  $U(x_i, \rho, f)$ , use is made of the direct and inverse two-dimensional FFT, respectively, instead of integration, according to formulas (23) and (24). The values of  $K$  and  $M$  determine the dimension of the three-dimensional arrays ( $K \times M \times M$ ) of the calculated complex values and the required RAM capacity. The frequency step  $\Delta f$  must satisfy the conditions  $\Delta f \ll \sigma_f$  and  $K\Delta f \gg \sigma_f$ . In calculating the random energy density  $W(L, \rho)$  according to formulas (25) and (28), integration of  $|U(L, \rho, f)|^2$  in  $f$  is replaced by summation over all  $k$ .

Using a sufficiently large number of independent numerically simulated realisations  $W(L, \rho)$ , we can evaluate various statistical characteristics of the radiation energy density, in particular, the average value  $\langle W(L, \rho) \rangle$  and relative variance  $\sigma_W^2$ :

$$\sigma_W^2(L, \rho) = \langle W^2(L, \rho) \rangle / \langle W(L, \rho) \rangle^2 - 1. \quad (32)$$

## 6. Results of numerical simulation

For the numerical simulation of random realisations  $W(L, \rho)$ , we set the following parameters:  $\lambda_0 = 1 \mu\text{m}$  ( $f_0 = 300 \text{ THz}$ ),  $\tau_p = 5 \text{ fs}$  ( $\tau_0 = 3 \text{ fs}$ ,  $\sigma_f = 53 \text{ THz}$ ),  $a_0 = 1.26 \text{ cm}$  (narrow beam) and  $5 \text{ cm}$ ,  $\infty$  (plane wave) and  $L = 1 \text{ km}$ . For such values of  $\lambda_0$  and  $\tau_0$  the emission spectrum is different from zero in the frequency range  $100\text{--}500 \text{ THz}$ , which corresponds to a wavelength range of  $0.6\text{--}3 \mu\text{m}$ . At each node of the computational grid with  $h = 2 \text{ mm}$  and  $M = 512$  the complex spectral amplitude values were calculated for 41 spectral channels having a width  $\Delta f = 10 \text{ THz}$ , i.e., in the discrete representation the frequency takes the values  $f = f_1 + k\Delta f$  at  $f_1 = 100 \text{ THz}$ ,  $k = 0, 1, \dots, K$  and  $K = 40$ .

In parallel with  $W(L, \rho)$  we calculated the spectral intensity  $S_I(L, \rho, f_0)$  and normalised intensity  $I_N(L, \rho) = S_I(L, \rho, f_0) / S_I(0, 0, f_0)$  of narrowband (cw) laser radiation. During the measurement time  $\Delta t$ , satisfying the condition  $f_p^{-1} \gg \Delta t \gg \tau_p(L)$  ( $f_p$  is the pulse repetition rate) in the case of pulses emission, the intensity  $I(L, \rho)$  of cw radiation with the frequency  $f_0$  does not change. Consequently, after normalisation to  $W(0, 0)|_{r_0=\infty}$  the energy density  $W(L, \rho)|_{r_0=\infty} = \Delta t I(L, \rho)$  measured during the time  $\Delta t$  is  $I_N(L, \rho)$ . Comparison of the normalised energy density  $W_N(L, \rho) = W(L, \rho) / W(0, 0)$  of pulsed radiation and the intensity  $I_N(L, \rho)$  of cw radiation for the

same generated array of random phase screens allows one to see the qualitative and quantitative difference between these characteristics in the same realisation.

Figures 1 and 2 show examples of random realisations of the normalised energy densities  $I_N(L, \rho)$  and  $W_N(L, \rho)$  of a beam with  $a_0 = 5 \text{ cm}$  at  $C_n^2 = 10^{-13}$  and  $10^{-12} \text{ m}^{-2/3}$ , respectively. One can see that the distribution of  $W_N(L, \rho)$  is smoother than that of  $I_N(L, \rho)$ . This difference is noticeable in Fig. 2, which presents the result of simulation in the case of strong turbulence.

### 6.1. Average energy density

Figure 3 illustrates the distribution of the normalised average energy density  $\langle W_N(L, \rho) \rangle$  with  $a_0 = 5 \text{ cm}$  in the absence of turbulence [curve (1)] and at  $C_n^2 = 10^{-12} \text{ m}^{-2/3}$  [curve (2) for cw radiation and curve (3) for pulsed radiation with  $\tau_p(0) = 5 \text{ fs}$ ]. At  $C_n^2 = 0$ ,  $L = 1 \text{ km}$ ,  $\lambda_0 = 1 \mu\text{m}$  and  $a_0 = 5 \text{ cm}$ , the distribution  $\langle W_N(L, \rho) \rangle$  does not depend on  $\tau_0$ . The presence of turbulence on the path leads to the fact that at  $C_n^2 = 10^{-12} \text{ m}^{-2/3}$  the effective beam radius of pulsed radiation with  $\tau_p(0) = 5 \text{ fs}$  is about 4% less than for narrowband (cw) radiation. The numerical simulation algorithm in question is applicable at  $\sigma_f/f_0 \ll 1$ , which does not allow the energy density distribution to be calculated at  $\sigma_f/f_0 > 1$ , when the effect of reducing the diffraction spreading of the beam manifests itself most strongly [13–17].

### 6.2. Energy density fluctuations

In the case of a plane wave (when we can put  $a_0 = \infty$  in the numerical simulation), the same values of  $\lambda_0$ ,  $\tau_0$  and  $L$ , which were set in the calculations in Figs 1 and 2, and  $C_n^2 = 10^{-12} \text{ m}^{-2/3}$ , from the array of simulated random realisations  $I_N(x_i, \rho)$  (cw radiation) and  $W_N(x_i, \rho)$  (pulsed radiation), where  $x_i = i\Delta x$ ,  $i = 0, 1, \dots, N$ ,  $\Delta x = 10 \text{ m}$ , and  $N = 100$ , we calculated the relative standard deviations of the radiation energy density fluctuations  $\sigma_W(x_i)$  using the data obtained from 100 independent statistical tests. Because the statistical characteristics do not depend on  $\rho$  in the plane wave regime, in averaging we used all the data generated by the computer at nodes of the  $512 \times 512$  computational grid. In this case, the calculation error  $\sigma_W(x_i)$  does not exceed 1%.

For cw radiation  $\sigma_W$  is nothing else than the standard deviation of the relative intensity fluctuations. The calculation results for  $\sigma_W$  as a function of the parameter

$$\beta_0 = \sqrt{1.23 C_n^2 (2\pi/\lambda_0)^{7/6} x_i^{11/6}}$$

characterising the optical turbulence intensity on the propagation path of length  $x_i$  [5–8] are shown in Fig. 4 in the form of curves (1) and (2). One can see that the values of  $\sigma_W$  for cw and pulsed radiation at  $\beta_0 \leq 1$  differ insignificantly. With increasing  $\beta_0$ , the standard deviation of the intensity in both cases, after reaching a peak in the vicinity of point  $\beta_0 = 2$ , decreases. In this case, curve (2) corresponding to the pulsed radiation decreases faster than curve (1) (cw radiation), and, starting from  $\beta_0 \approx 3.3$ , the standard deviation of  $\sigma_W$  for pulsed radiation becomes less than unity. At the same time,  $\sigma_W$  for cw radiation at  $\beta_0 > 1$  is greater than unity, and in the limit  $\beta_0 \rightarrow \infty$  tends to unity [6–8].

For a plane wave the average value of the spectral intensity  $S_I(x_i, \rho, f)$  is independent of  $(x_i, \rho)$  and determined by the

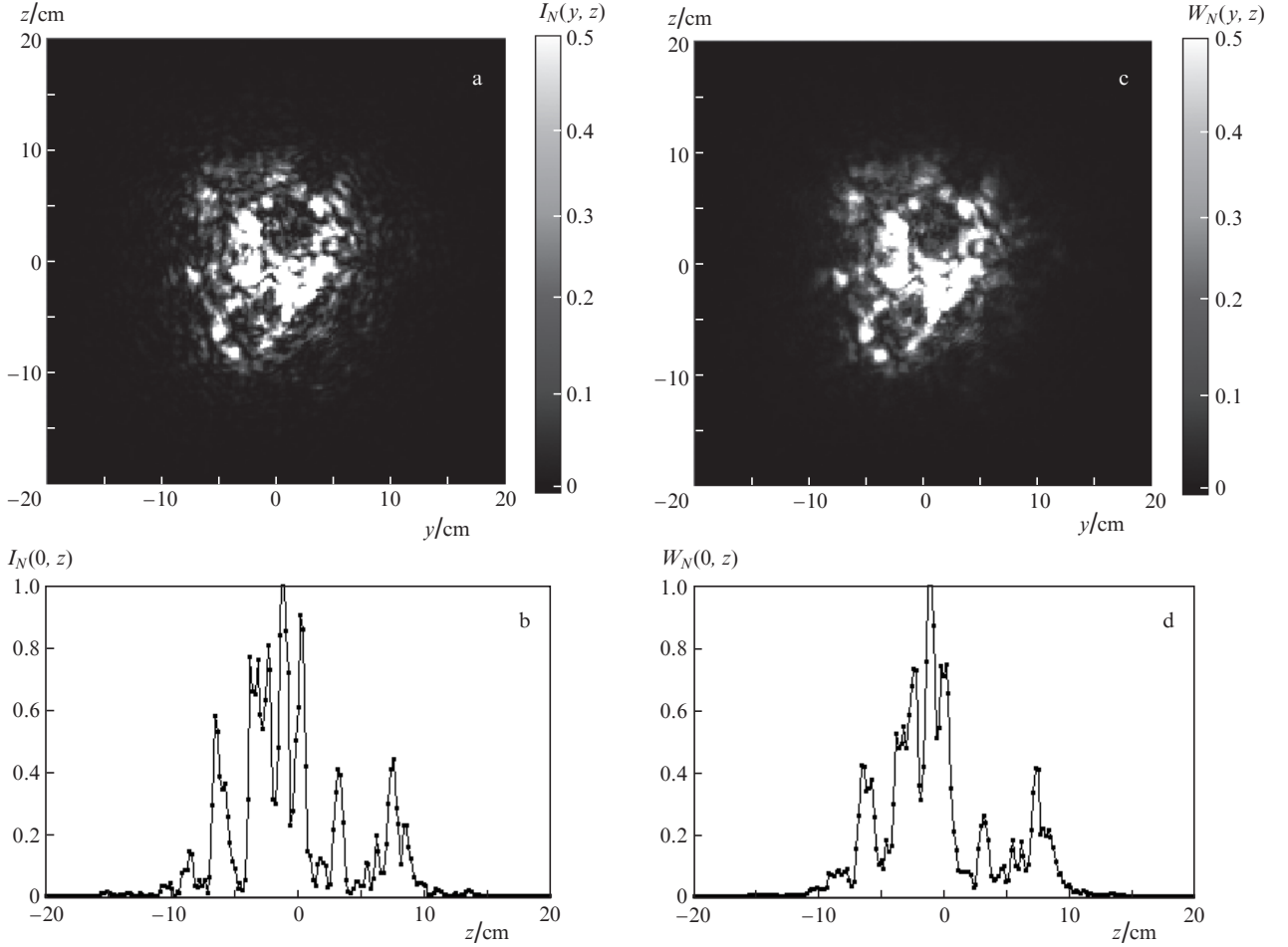


**Figure 1.** (a, c) Two-dimensional and (b, d) one-dimensional distributions of the normalised energy densities of (a, b) cw and (c, d) pulsed radiation at  $C_n^2 = 10^{-13} \text{ m}^{-2/3}$ .

expression  $\langle S_I(f) \rangle = |\tilde{E}(0, \boldsymbol{\rho}, f)|^2$  at  $a_0 = \infty$  [see Formula (4)], and the relative variance of the energy density  $\sigma_W^2(x_i, \boldsymbol{\rho})$  depends only on  $x_i$ . Then from (28) and (32) we have

$$\sigma_W^2(x_i) = (\sqrt{\pi} \tau_0 E_0^2)^{-2} \times \int_{-\infty}^{+\infty} df_1 \int_{-\infty}^{+\infty} df_2 \langle S_I(f_1) \rangle \langle S_I(f_2) \rangle K_s(x_i, f_1, f_2), \quad (33)$$

where  $K_s(x_i, f_1, f_2) = \langle s(x_i, \boldsymbol{\rho}, f_1) s(x_i, \boldsymbol{\rho}, f_2) \rangle$  is the frequency correlation of normalised intensity fluctuations  $s(x_i, \boldsymbol{\rho}, f) = S_I(x_i, \boldsymbol{\rho}, f) / \langle S_I(f) \rangle - 1$ . It follows from the experiment [21] that with the growth of  $\beta_0$  in the range from 0 to 1, the ratio  $K_s(x_i, f_1, f_2) / K_s(x_i, f, f)$ , where  $f = (f_1 + f_2) / 2$  and  $f_1 \neq f_2$ , is close to unity and decreases at  $\beta_0 > 1$ . Therefore, in view of (33) with  $2\sigma_f / f_0 = 0.353$  in the region of strong intensity fluctuations when the parameter  $\beta_0 \gg 1$ , the level of the energy density fluctuations is significantly lower in the case of a pulse with a duration  $\tau_0 = 3 \text{ fs}$  than for narrowband radiation ( $\tau_0 \rightarrow \infty$ ).

In the process of numerical simulation of the femtosecond pulse propagation in a turbulent atmosphere, one can observe on the computer how the shape of the spectrum  $S_I(x_i, \boldsymbol{\rho}, f)$  changes with increasing  $i$  at fixed  $\boldsymbol{\rho}$ . As radiation propagates, the characteristic frequency scaling  $f_T$  of spectrum fluctuations at  $\beta_0 > 1$  decreases, so that after integration over  $f$  in

(28) the fluctuations of the radiation energy density are partially averaged. In the limit when  $\beta_0 \rightarrow \infty$ , the ratio  $f_T / \sigma_f \rightarrow 0$  and, therefore,  $\sigma_W \rightarrow 0$ , unlike cw radiation for which  $\sigma_W \rightarrow 1$ . The effects of de-correlation of strong intensity fluctuations of frequency separated waves and averaging of partially coherent cw radiation in a turbulent atmosphere have been previously described in [22–24].

To construct curve (2) in Fig. 4, we performed numerical simulations in 41 frequency channels ( $K = 40$ ) of width  $\Delta f = 10 \text{ THz}$  each. However, under certain conditions, the scaling  $f_T$  can be less than  $\Delta f$ . We increased twice the number  $K$  at a constant frequency range  $K\Delta f$ , centred with respect to point  $f_0$ , and obtained a result similar to that shown by curve (2) in Fig. 4. Thus, for those  $\beta_0$  at which we plotted the curve, it is sufficient to use 41 frequency channels.

Curves (3) and (4) in Fig. 4 show the results of numerical simulation for the case of a narrow collimated beam when the Fresnel number  $\Omega = 2\pi a_0^2 / (\lambda_0 L) = 1$ . These curves represent standard deviations of relative energy density fluctuations of cw and pulsed radiation with  $\lambda_0 = 1 \mu\text{m}$  on the optical axis ( $\boldsymbol{\rho} = 0$ ). Because in the simulation using 20 layers we set  $L = 1 \text{ km}$  ( $N = 20$ ,  $\Delta x = 50 \text{ m}$ ), then for the Fresnel number to be equal to unity at the path's end, we should set  $a_0 = 1.26 \text{ cm}$ . In this case, we could use for  $\sigma_W(\beta_0)$  calculations only  $I_N(x_i, \boldsymbol{\rho})$  and  $W_N(x_i, \boldsymbol{\rho})$ , generated at the end of the propagation path ( $x_i = L$ ). Therefore, to calculate  $\sigma_W$  at different  $\beta_0$ , we changed appropriately the value of  $C_n^2$ . We used 1000 independent sta-

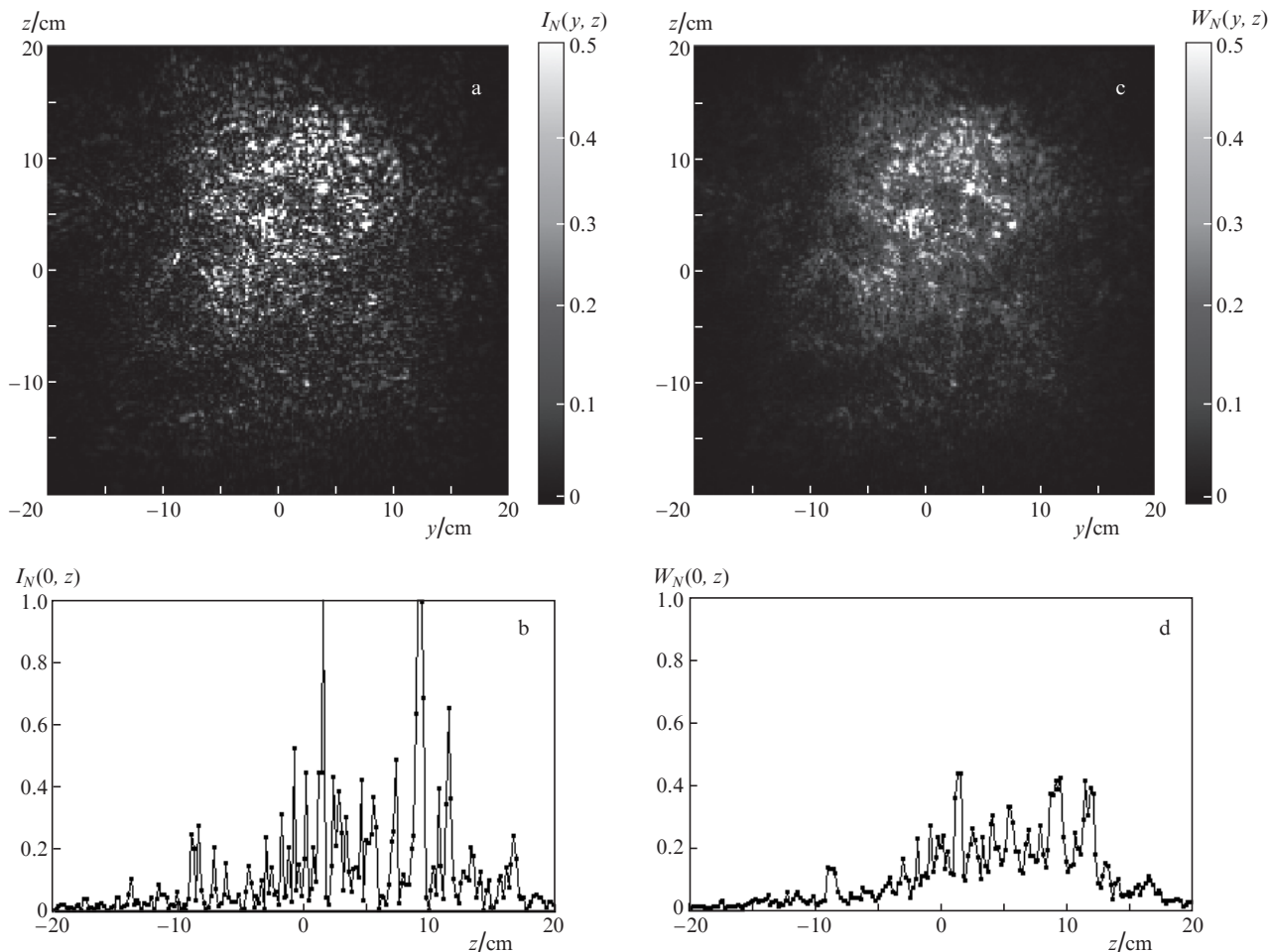


**Figure 2.** (a, c) Two-dimensional and (b, d) one-dimensional distributions of the normalised energy densities of (a, b) cw and (c, d) pulsed radiation at  $C_n^2 = 10^{-12} \text{ m}^{-2/3}$ .

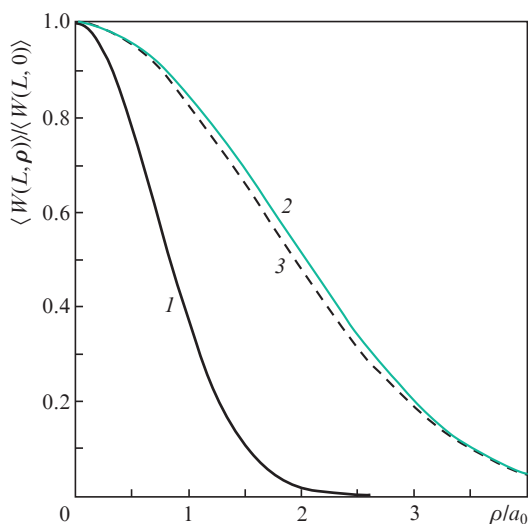


**Figure 3.** Distribution of the normalised average energy density of laser radiation in a plane transverse to the optical axis at  $C_n^2 = 0$  (1) and  $10^{-12} \text{ m}^{-2/3}$  for narrowband radiation (2) and a pulse with a duration of 5 fs (3).

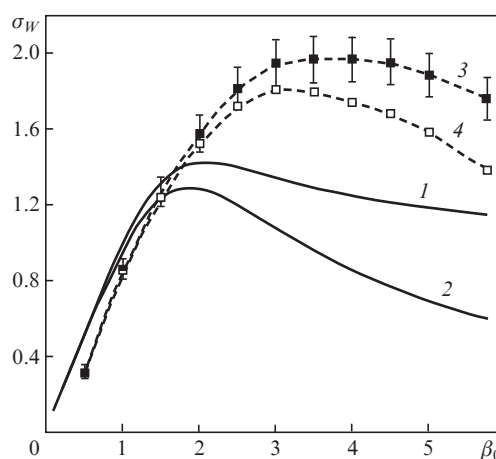


**Figure 4.** Standard deviations of relative energy density fluctuations of cw radiation (1, 3) and pulsed radiation with a pulse duration  $\tau_p(0) = 5 \text{ fs}$  (2, 4) in the regimes of a plane wave (1, 2) and a narrow collimated beam at  $\Omega = 1$  (3, 4) vs.  $\beta_0$ . The errors correspond to a 95% confidence interval.

tistical tests. Note that in simulating random phase screens for a narrow beam with  $\Omega = 1$ , we used the method of sub-harmonics [19, 20], which was not required for a plane wave.

According to the results shown in Fig. 4, in the case of a narrow collimated beam (and a plane wave), the difference in the levels of cw and short-pulsed radiation fluctuations increases with increasing  $\beta_0$ . Moreover, a marked decrease in

$\sigma_W$  at  $\tau_p(0) = 5$  fs with respect to cw radiation occurs at  $\beta_0 > 2$ . One can see that compared to a plane wave, the effect of de-correlation of intensity fluctuations at different frequencies is less pronounced in the case of a narrow beam. The fact is that, as the analysis of the simulated data showed, the frequency averaging of energy density fluctuations is equivalent to the action of a spatial low-frequency filter, and the higher the value of  $\beta_0$  in the region of strong intensity fluctuations at a wavelength of  $\lambda_0$ , the less their characteristic scale and hence the greater the averaging. In the case of a spatially limited beam with  $\Omega = 1$  and not too large  $\beta_0$  (e.g.,  $\beta_0 < 4$ ), an essential contribution to the energy density (and intensity) fluctuations is made by random lateral displacements of the laser beam as a whole, which are virtually not averaged due to frequency de-correlation.

## 7. Conclusions

We have proposed an algorithm of computer simulation of short-pulse laser radiation propagation in a turbulent atmosphere on the basis of the solution of the parabolic wave equation for the complex spectral amplitude of the wave field by the split-step method. The algorithm allows the study of statistical characteristics of the energy density of short-pulse radiation as a function of diffraction and turbulent conditions on the propagation path. By using the proposed algorithm we have calculated the dependence of the variance  $\sigma_W^2$  of energy density fluctuations of a femtosecond pulse propagating in the atmosphere in the plane wave regime on the parameter  $\beta_0$  characterising the turbulent propagation conditions. It is shown that with increasing optical turbulence (a growth of  $\beta_0$ ), the dependence  $\sigma_W(\beta_0)$  for pulsed radiation becomes significantly different from the known dependence of the standard deviation of the plane wave intensity  $\sigma_I(\beta_0)$  for cw radiation. In the limit  $\beta_0^2 \rightarrow \infty$ ,  $\sigma_W(\beta_0) \rightarrow 0$ , whereas  $\sigma_I(\beta_0) \rightarrow 1$ .

The algorithm can be generalised to the case of an arbitrary spatiotemporal initial amplitude and phase distribution of the beam of pulsed radiation. It can also be used for the numerical study of the propagation of pulsed radiation on the laser detection and ranging [25, 26].

**Acknowledgements.** This work was financially supported by the Russian Foundation for Basic Research (Grant No. 13-02-98016-r\_sibir).

## References

1. Apeksimov D.V., Bagayev S.N., Geints Yu.E., Zemlyanov A.A., Kabanov A.M., Kirpichnikov A.V., Kistenev Yu.V., Krekov G.M., Matvienko G.G., Oshlakov V.K., Panina E.K., Petrov V.V., Pstryakov E.V., Ponomarev Yu.N., Sukhanov A.Ya., Tikhomirov B.A., Trunov V.I., Uogintas S.R., Frolov S.A., Khudorozhkov D.G. *Femtosekundnaya atmosfer'naya optika* (Femtosecond Atmospheric Optics) (Novosibirsk: Izd-vo SO RAN, 2010).
2. Kandidov V.P., Kosarev O.G., Tamarov M.P., Brodeur A., Chin S. *Kvantovaya Elektron.*, **29**, 73 (1999) [*Quantum Electron.*, **29**, 911 (1999)].
3. Shlenov S.A., Fedorov V.Yu., Kandidov V.P. *Opt. Atmos. Okeana*, **20**, 308 (2007).
4. Kandidov V.P., Shlenov S.A. *Opt. Atmos. Okeana*, **25** (1), 11 (2012).
5. Tatarskii V.I. *Rasprostraneniye voln v turbulentnoi atmosfere* (Wave Propagation In A Turbulent Atmosphere) (Moscow: Nauka, 1967).
6. Gurvich A.S., Kon A.I., Mironov V.L., Khmelevtsov S.S. *Lazernoe izlucheniye v turbulentnoi atmosfere* (Laser Radiation In A Turbulent Atmosphere) (Moscow: Nauka, 1976).
7. Rytov S.M., Kravtsov Yu.A., Tatarskii V.I. *Vvedeniye v staticheskuyu radiofiziku. Chast' II. Sluchainyye polya* (Introduction to Statistical Radiophysics. Part II. Random Fields) (Moscow: Nauka, 1978).
8. Zuev V.E., Banakh V.A., Pokasov V.V. *Sovremennyye problemy atmosferno optiki* (Modern Problems of Atmospheric Optics) (Leningrad: Gidrometeoizdat, 1988) Vol. 5.
9. Kandidov V.P. *Usp. Fiz. Nauk.*, **166**, 1309 (1996).
10. Akhmanov S.A., Vysloukh V.A., Chirkin A.S. *Optics of Femtosecond Laser Pulses* (New York: AIP, 1992; Moscow: Nauka, 1988).
11. Christov I.P. *Opt. Commun.*, **53**, 364 (1985).
12. Christov I.P. *Opt. Acta*, **33**, 63 (1986).
13. Zaloznaya I.V., Falits A.V. *Opt. Atmos. Okeana*, **22**, 734 (2009).
14. Banakh V.A. *Opt. Lett.*, **36**, 4554 (2011).
15. Gerasimov L.O., Zaloznaya I.V. *Opt. Atmos. Okeana*, **24**, 185 (2011).
16. Banakh V.A., Gerasimov L.O., Zaloznaya I.V., Tikhomirov O.V. *Opt. Atmos. Okeana*, **25**, 941 (2012).
17. Banakh V.A., Gerasimov L.O. *Opt. Atmos. Okeana*, **26**, 5 (2013).
18. Banakh V.A., Smalikho I.N. *Coherent Doppler Wind Lidars in a Turbulent Atmosphere* (Boston – London: Artech House, 2013).
19. Frehlich R. *Appl. Opt.*, **39**, 393 (2000).
20. Banakh V.A., Smalikho I.N., Falits A.V. *Opt. Atmos. Okeana*, **24**, 848 (2011).
21. Gurvich A.S., Kan V. *Izv. Vyssh. Uchebn. Zaved., Ser. Radiofiz.*, **22**, 843 (1979).
22. Zavorotnyi V.U. *Izv. Vyssh. Uchebn. Zaved., Ser. Radiofiz.*, **24**, 601 (1981).
23. Banakh V.A., Buldakov V.M., Mironov V.L. *Opt. Spektrosk.*, **54**, 1054 (1983).
24. Banakh V.A., Buldakov V.M. *Opt. Spektrosk.*, **55**, 707 (1983).
25. Banakh V.A., Smalikho I.N. *Opt. Atmos. Okeana*, **24**, 300 (2011).
26. Smalikho I.N. *Opt. Atmos. Okeana*, **25**, 796 (2012).